published in Environmental Science and Technology 52 (2018) 4163−4172 reprints also to galceran@quimica.udl.cat

Metal (Pb, Cd, Zn) binding to diverse organic matter samples and implications for speciation modelling

Weibin Chen†, Céline Guéguen#,, D. Scott Smith§, Josep Galceran‡, Jaume Puy‡, Encarnació Companys‡*

† Environmental & Life Science program, Trent University, Peterborough, Ontario, Canada

Department of Chemistry, Trent University, Peterborough, Ontario, Canada

§ Department of Chemistry & Biochemistry, Wilfrid Laurier University, Waterloo, Ontario, Canada

Abstract

This study evaluated the influence of dissolved organic matter (DOM) properties on the speciation of Pb, Zn and Cd. Six DOM samples were categorized into autochthonous and allochthonous source based on their absorbance and fluorescence properties. The concentration of free metal ions (C_M^{2+}) measured by titration using Absence of Gradient and Nernstian Equilibrium Stripping (AGNES) was compared with that predicted by Windermere Humic Aqueous Model (WHAM). At the same binding condition (pH, dissolved organic carbon, ionic strength, and total metal concentration) the allochthonous DOM showed a higher level of Pb binding than the autochthonous DOM (84- to 504-fold C_{Pb}^{2+} variation). This dependency, however, was less pronounced for Zn (12- to 74-fold C_{Zn}^{2+} variation) and least for Cd (2- to 14-fold C_{Cd}^{2+} variation).

The WHAM performance was affected by source variation through the active DOM fraction (F). The commonly used F = 1.3 provided reliable C_{Pb}^{2+} for allochthonous DOMs and acceptable C_{Cd}^{2+} for all DOM, but significantly underpredicted C_{Pb}^{2+} and C_{Zn}^{2+} for autochthonous DOM. Adjusting F improved C_M^{2+} predictions, but the optimum F values were metal-specific (e.g., 0.03 – 1.9 for Pb), as showed by linear correlations with specific optical indexes. The results indicate a potential to improve WHAM by incorporating rapid measurement of DOM optical properties for site-specific F.

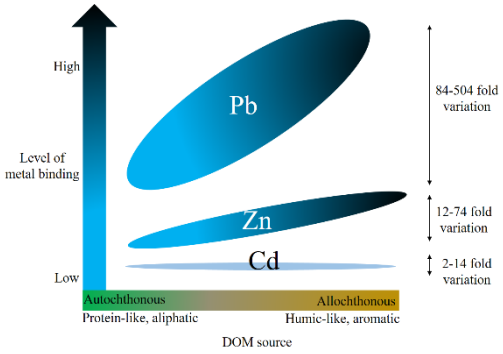

Introduction

Dissolved organic matter (DOM) is ubiquitous in natural waters and plays an essential role in regulating metal speciation and toxicity. In most cases, the free metal ion is the most toxic species, and its binding to DOM can alleviate metal toxicity.[1–4] The binding reaction is affected by water chemistry (*i.e.*, competitive ions, pH, ionic strength, and mineral oxides) and DOM properties.[5] The water chemistry is relatively easy to characterize or define. The description of DOM properties, however, is challenged by the heterogeneity regarding composition, structures, and molecular weight[6,7] of DOM and their effects on metal binding.[8–11]

The Windermere Humic Aqueous Model (WHAM) is used to predict the concentration of free metal ions (*e.g.*, C_M^{2+} for divalent metal ion) for toxicity assessments by Biotic Ligand Model (BLM).[12–14] WHAM assumes the stability constants are independent of DOM heterogeneities,[15,16]

but the binding site capacity varies between DOM samples. WHAM calculates the binding site capacity based on the concentration of dissolved organic carbon (C_{DOC}) and the active fraction of DOM participating in metal binding (F; F = C_{ADOM} / C_{DOC}, where C_{ADOM} is the concentration of active DOM for metal binding).[17] Unlike C_{ADOM}, the C_{DOC} can be experimentally determined. A reliable metal toxicity assessment by BLM, therefore, partially relies on the use of adequate C_{ADOM} and F value in WHAM. For Cu, Bryan and coworkers[18] determined the geometric mean of different F values for 15 UK surface waters was 1.3. Since then, F = 1.3 has been widely used by WHAM users, even though the DOM properties may vary with sources and the metals of interest may not be Cu.[13,14,17,19,20] In fact, numerous studies[12,19,21–24] have shown that the level of Cu-binding increased with increasing allochthonous characteristics (*i.e.,* increasing aromaticity, humic-like component, and optical color), suggesting the necessity of adjusting F to improve $C_{Cu^{2+}}$ predictions for specific DOM samples. Some studies[12,25,26] have found that the optimal F (F_{opt}) values correlated linearly with DOM property surrogates based on absorbance and fluorescence for Cu (*e.g.,* aromaticity[12,25]or abundance of fluorescent humic-like components[26]). To derive these correlations, studies carefully designed to measure and compare $C_{M^{2+}}$ between different DOM are indispensable.

However, the evaluation of DOM properties on the binding of toxic metals, including Pb,[24,27–30] Zn,[31,32] and Cd,[3,8,24]are limited. Town et al.[16] extensively reviewed the variation of Pb-binding affinity between different isolated humic substances and biota-derived materials, implying the property effects of organic matter on Pb-binding. More recent studies have found the hydrophobicity[33] and the abundance of fluorescent humic-like components[34] were significantly influencing Pb-binding. Nonetheless, all the studies mentioned above were limited to isolated humic substances,[16,35] biota-derived materials,[16] leachates of sewage[34] or organic matter from

wastewater effluents.[33] Whether these organic matters can represent the natural DOM, however, remains unclear.[16] Only few studies compared the level of Zn-binding between different natural DOM and inconsistent results were reported, likely due to different methods to characterize and differentiate DOM samples, different extents of DOM property variation, and different binding conditions. For example, Cheng and Allen[15] found a similar level of Zn-binding between three surface water DOM samples with different geographic locations, dissolved organic and inorganic carbon concentrations. Contrarily, Muller et al[26] determined the absorbance and fluorescence characteristics of eleven Canadian lake DOM samples and found the level of Zn-binding significantly decreased with increasing allochthonous feature. Cheng et al.[36] also reported a varying degree of Zn-binding between five freshwater DOM, but the observed variation was possibly not due to the variation of DOM properties alone because of different binding conditions (*i.e.*, varying DOC, pH, and hardness). On the other hand, the evaluation of DOM property effects on Cd binding are relatively more limited. Xue and Sigg[37,38] concluded the variation of Cd-binding between three lakes was linked to the variation of biological primary productivity; no specific DOM or water chemistry characterization, however, was performed. Mueller et al.[26] attributed the variation of Cd-binding between 11 lake DOM to the varying abundances of fluorescent humic-like components. However, in their study, the effects of DOM properties on Cd-binding were not explicitly isolated from the impacts of water chemistry, including DOC, pH, and hardness.[39] Another challenge is the method used to estimate C_M^{2+}, including Anodic stripping voltammetry (ASV)[15,36,38] and competitive ligand exchange adsorptive cathodic stripping voltammetry (CLE-AdCSV).[37] ASV not only measures M^{2+} but also other labile metal species,[40] whereas CLE-AdCSV requires complicated equilibrium and kinetic consideration,[40,41] which makes the comparison with the WHAM-predicted C_M^{2+} less straight forward.

In this study, we experimentally determined and compared the metal speciation (*i.e.*, Pb, Zn, and Cd) between six different DOM from surface waters. The DOM properties were characterized by four techniques, including the fluorescence excitation-emission matrix (FEEM), absorbance, potentiometric titrations, and Cr-reducible-sulfide (CRS). The FEEM allows us to rapidly obtain the optical spectroscopic DOM components for sample differentiations.[42] The absorbance provides a convenient way to estimate the aromaticity[43] and molecular sizes[44] of DOM, important physicochemical factors affecting metal binding.[11,12] The potentiometric titrations determine the abundances of DOM functional groups.[45,46] The CRS method was used to determine the concentration of reduced sulfides,[47,48] thought to be representative of strong metal binding sites.[49] These techniques, particularly the FEEM and absorbance, are accessible, rapid, and well-accepted.[42] More importantly, the property data measured by these techniques are relatively simple to process, and therefore, can be potentially integrated into the WHAM model. Metal titrations, rather than one-point speciation,[26] were performed to determine the metal binding to various ligands on DOM molecules (*e.g.*, from weak to strong ligand: carboxylic, phenolic, reduced sulfur or other multidentate)[16,49,50] under fixed DOC concentration, pH and ionic strength. Absence of Gradient and Nernstian Equilibrium Stripping (AGNES) was employed to measure the C_M^{2+} (*i.e.* C_{Pb}^{2+}, C_{Zn}^{2+}, and C_{Cd}^{2+}),[35,51,52] which allows us to make direct comparisons with the WHAM-predicted C_M^{2+} and determine F_{opt}.

Specifically, this study aimed to 1) evaluate the effect of DOM properties on Pb-, Cd-, and Zn-binding ; 2) investigate the reliability of using F = 1.3 to predict C_M^{2+} for site-specific DOMs and metals other than Cu; 3) derive potential correlations between the F_{opt} and measurable DOM properties. The results of this study will show a potential of integrating DOM property parameters into WHAM for predicting C_M^{2+} where organic matter quality varies significantly.

Materials and methods

Collection of different DOM samples

Natural DOM samples were collected from five different sites, including Desjardin Canal (DC; N 43°15'59.2308"N, W 079°56'33.8280"), Burlington Bay (BBL; N 43°18'03.3984", W 079°50'42.3528"), Amazon River (AMR; S 3°5'41.5", W 60°21'19.6"), Bannister Lake (BL; N $43^0$30'N, W $80^0$38'), and Luther Marsh (LM; N $43^0$39', W $80^0$26'). At each site, the raw water sample was first filtered through a 1 μm pore-size filter, and then concentrated by reverse osmosis (RO).[53] The RO technique has been shown to preserve DOM integrity.[54] The RO-DOM concentrates were immediately transported back to the lab where they were treated by cation exchange resins (AG50W-X8, H^+ form, BioRad, Richmond, CA, USA) to remove background metal ions.[24] Briefly the resins were activated by 4 mol L^{-1} HCl, followed thoroughly rinsing with milli-Q water (MQW; resistance ≥ 18 MΩ cm^{-1} and C_{DOC} < 3 ppb; Millipore) before usage. To prevent humic acid precipitation, the final pH of DOM samples after resination was adjusted to 2–3. All RO-DOM concentrates were stored at 4^0 C in darkness until use. Because of the addition of hydrochloric acid during resination, the concentration of chloride ion (C_{Cl^-}) in RO-DOM concentrates were determined by the chloride ion selective electrode (Mantech, PCE80-Cl-1001) to assess the concentrations of metal-chloride species.

The Suwannee River Humic Acid (SRHA) standard was also used to represent allochthonous DOM. The SRHA (i.e. 1S101H) was purchased from International Humic Substance Society and used without pretreatment.

Characterization of DOM properties

The FEEM and absorbance were measured at 10 mg L^{-1} DOC at pH 8.0 (Supplementary information (SI), page S1). The FEEMs were operationally delimitated into three fluorescence regions that represent different DOM components[55]: protein-like component at Ex250-

300/Em300-400 (C1), terrestrially-derived humic-like component at Ex250-300/Em400-600 (C2), and humic-like component at Ex300-500/Em400-600 (C3). The '-like' term means the fluorescence properties of these components resemble that of pure humic, fulvic, and protein materials. The relative abundances of each component (C1%–C3%) were estimated by integrating the volume under the respective fluorescent peaks (SI, page S2).

Different component or source indices were used: the abundance ratio of humic-like to protein-like component (Hum/Pro = (C2% + C3%) / C1%), fluorescence index (FI = fluorescence intensity$_{EX370nm/\ Em450nm}$/fluorescence intensity$_{Ex370nm/\ Em500nm}$),[56] and autochthonous contribution index (BIX = fluorescence intensity$_{310nm\text{-}excitation\ and\ 380nm\text{-}emission}$ / fluorescence intensity$_{310nm\text{-}excitation\ and\ 430nm\text{-}emission}$).[57] The autochthonous feature increases with increasing BIX value.[57]

Different indicators based on absorbance measurements were used to estimate DOM properties. The DOM aromaticity was estimated by the specific absorbance coefficient at 254, 340, and 436 nm (*i.e.* $SUVA_{254}$ = 2.303×absorbance at 254 nm / C_{DOC}, SAC_{340} = 2.303×absorbance at 340 nm / C_{DOC}, and $SCOA_{436}$ = 2.303×absorbance at 436 nm / C_{DOC}).[43,58,59] The $SUVA_{254}$ and SAC_{340} values increase with increasing DOM aromaticity.[43,58] The $SCOA_{436}$ value increases with increasing yellow-brown colored moieties.[58] The molecular weight of DOM was estimated by the ratio of absorbance at 254 nm to that at 365 nm (Abs_{254}/Abs_{365}),[59] and the ratio of spectral slope at 275–295 nm to that at 350–400 nm (S_R).[44] The Abs_{254}/Abs_{365} and S_R decrease with increasing molecular weight.[44,59]

The proton reactivity was determined by potentiometric titration (SI; page S2). The proton binding affinity spectra (*i.e.* site capacity ($L_{T\text{-}H}$) vs. site affinity (pK_a)) were determined by optimally fitting the deprotonation data (*i.e.* pH vs. overall charge density) to a continuous-site model through a Fully Optimized ContinUous (FOCUS) procedure.[45] Based on the affinity

spectrum, the proton sites were categorized into three groups: acidic site (pKa ≤ 5), intermediate site (5 < pKa ≤ 8.5), and basic site (pKa > 8.5), representing the deprotonation of carboxylic and phenolic groups as pH increases.[60] The total capacity ($L_{T\text{-}H}$; μmol mg-C^{-1}) was calculated by integrating the area within their pKa ranges. A Proton Binding Index was calculated (PBI= $L_{T\text{-}H}$ at intermediate site / ($L_{T\text{-}H}$ at acid site + $L_{T\text{-}H}$ at basic site)/2).[58] The PBI index is thought to increase with increasing potential of DOM to form strong metal complexes.[58]

A hierarchical clustering analysis was used to group the samples based on similar absorbance and fluorescence DOM properties (SI, page S3).[21] The accuracy of the clustering was described by a cophenetic correlation coefficient (*i.e.* the closer to 1, the more accurate), and the dissimilarity level between samples was described by an inconsistency coefficient (*i.e.* the larger, the more distinct).

Metal titration

Metal titrations were performed with low DOM concentration.[16,33] The pH = 8.0 was selected because it makes the deprotonation of most binding sites within environmentally relevant pH range.[61] The pH = 8.0 also makes most of the binding sites deprotonated. For all samples, a 100-mL DOM solution containing C_{DOC} = 10 mg L^{-1} and 0.1 M KNO_3 electrolyte was prepared by appropriate dilution of RO-concentrate with MQW and dissolution of KNO_3 salt (Sigma; purity > 99%). The 100-mL DOM solution was then transferred to a 200-mL glass vessel for titration experiments. The pH of the DOM solution was consistently monitored by a micro-pH electrode (Manteq, PCE-80-PH1020MIC). The initial pH before adjustment was around 2-3. Under this acidic condition, the DOM solution was consistently purged with high-purity N_2 for 5-10 minutes to remove all HCO_3^-/CO_3^{2-} species. Then the pH was fixed to 8.0 for the entire titration and AGNES experiment by additions of microliter HNO_3 or NaOH (*i.e.* 0.1, 1, or 5 mol L^{-1}). Additionally, to prevent CO_2 and O_2 dissolution, the voltammetric vessel was seal and the

headspace was filled with high-purity N_2. Increasing amounts of metal titrants were added to reach a total metal concentration ($C_{M,T}$) ranging from $10^{-8.5}$ to $10^{-4.0}$ mol L^{-1} (*i.e.*, $10^{-0.25}$ mol L^{-1} increment; the total accumulative volume of metal titrant < 0.5 ml). The metal titrant solutions were 0.1−100 ppm Pb, Cd, or Zn, prepared by appropriate dilutions of 1000 ppm AAS standard solutions (Sigma Aldrich) with 2% double-distilled HNO_3. The total accumulative titrant volume was ≤ 3% of the sample volume and dilution effects were corrected accordingly. The $C_{M,T}$ range approximately corresponded to a metal:DOM ratio (mg/mg) increasing from 1:10000 to 1:10, which enabled us to determine metal binding to various ligands with orders of magnitude differences in binding affinity (*i.e.* from strong to weak).[61,62] Following each metal addition, the AGNES procedure was implemented to measure C_M^{2+}.

AGNES measurement of C_M^{2+}

The experimental specifications of the AGNES procedures for measuring C_M^{2+} were summarized in the SI (page S4–S5). The method has been preliminarily tested by measuring the C_{Pb}^{2+}, C_{Cd}^{2+}, and C_{Zn}^{2+} in the presence of tryptophan over a pH range from 2.0 to 8.5. Good agreements of C_M^{2+} were achieved between AGNES measurements and model predictions (Figure S1), validating the reliability of the method.

WHAM prediction of C_M^{2+}

The C_M^{2+} at each titration point was predicted by WHAM (Version 7.0.4, Centre for Ecology & Hydrology, Natural Environment Research Council, UK) with inputs of C_{DOC} = 10 mg L^{-1}, pH = 8.0, ionic strength = 0.1 M KNO_3, $C_{M,T}$ ($10^{-8.5}$–$10^{-4.0}$ mol L^{-1}), and C_{Cl^-} (*i.e.*, C_{Cl^-} = 0, 7.4, 5.4, 20.3, 61.7, and 79.6 mmol L^{-1} for SRHA, LM, ARM, BL, BBL, and DC, respectively). No background metal was considered because of the resination treatment.[24] The original concentration of $C_{NO_3^-}$ was assumed to be negligible due to the low $C_{NO_3^-}$ in Canadian rivers and lakes (*i.e.*, <

0.06 mmol L^{-1});[63] thus, nitrate concentration was equal to the ionic strength buffer value of 0.1 mol L^{-1}. The actual concentration of SO_4^{2-} (C_{SO4}^{2-}) in DOM samples was not measured. However, within the C_{SO4}^{2-} range in Canada (*i.e.* C_{SO4}^{2-} = 0-6 mmol L^{-1} for natural and contaminated surface waters[64]), modeling tests (SI, page S6) showed the impact of SO_4^{2-} on Pb-, Zn-, and Cd-binding was negligible (SI, Figure S2-S4). Therefore, the C_{SO4}^{2-} was not considered as a WHAM input in this study. Although the carbon content may vary between samples, all DOMs were assumed to contain 50% DOC by mass[65] and comprised of 100% fulvic acid[26] (except the SRHA) to keep consistency with previous studies [13,18,2613,18,26]. The SRHA was set to contain 100% humic acid. The usual default F value (F_{def}=1.3) was first used. The optimal F value (F_{opt}) was then determined by iteratively adjusting F until the overall difference in C_M^{2+} between the AGNES measurements and WHAM predictions was minimized. The overall difference was described by the Root Mean Squared Error (RMSE) term (Equation (1); *n* is the total number of metal titration points, and *i* is a specific titration point). The RMSE for F_{def} and F_{opt} is $RMSE_{def}$ and $RMSE_{opt}$, respectively.

$$\mathrm{RMSE} = \sqrt{\frac{1}{n}\sum_{i=1}^{n}(\log C_{\mathrm{M}^{2+},i,\mathrm{measured}} - \log C_{\mathrm{M}^{2+},i,\mathrm{WHAM}})^2} \quad (1)$$

Results and discussions

DOM properties

The DOM property parameters and indices are summarized in Table S1. Based on the FEEMs (Figure S5) the abundance of humic-like components (C2%+C3%) varied by a factor of 1.5 between DOM samples (70.3%–94.7%), whereas the protein-like component abundance (C1%) varied by a factor of 6 (5%–30%). The Hum/Pro varied by a factor of 7.6 (2.36–17.93). These component-relevant parameters indicate that the variability in the protein-like component is greater than that of the humic-like component. The FI value varied from 0.85–1.28, within the range

previously reported for freshwater aquatic DOM spanning from autochthonous to allochthonous source –2.31 [26,54]). However, the higher end of FI range in our study was smaller than that of previous study (*i.e.,* 2.13),[54] indicating our DOM samples were relatively more terrestrially-derived.[66] The BIX value varied within a range of 0.33–1.22, indicating varying degree of autochthonous features.[57] Although direct comparisons of BIX variation range for freshwaters were not available, our BIX range was comparable with the BIX range for estuarine waters (*i.e.* 0.65–0.95[57]). Together these fluorescence parameters indicated the DOM samples were within a gradient ranging from more autochthonous to more allochthonous source, although the distinction (by fluorescence) is not as large as that from previous studies.[54]

The $SUVA_{254}$ and SAC_{340} varied by a factor of 3.50 (*i.e.* 4.04–13.97) and 7.29 (*i.e.* 0.86–6.27), respectively, indicating the variation of DOM aromaticity.[43,46] The $SCOA_{436}$ varied by a factor of 11.7 (*i.e.* 0.15–1.75), showing the variation of the colored moieties.[67] The S_R and Abs_{254}/Abs_{365} varied by a factor of 3.48 (*i.e.* 1.89–4.53) and 2.61 (*i.e.* 3.3–7.66), respectively, showing variation of molecular weight.[59,68] Comparable variation factors have been also reported by previous studies for DOMs spanning from autochthonous to allochthonous source (*i.e.,* 2–3.16 for $SUVA_{254}$,[12,26,46,61,69] 1.18–11.93 for SAC_{340},[46,54] 7.8 for $SCOA_{436}$,[46] 3.48 for S_R,[69] and 2.62 for Abs_{254}/Abs_{365}[59]).

The proton binding affinity spectrum was only determined for SRHA, LM, AMR, and BL because the C_{DOC} of the RO-concentrates from BBL and DC were too low to provide reproducible titration data (*i.e.* $C_{DOC} \leq 81$ mg L^{-1}) (Figure S6). The total and group-specific (*i.e.* acidic, intermediate, and basic) proton-binding site capacity varied between samples. The PBI values varied from < 0.21 to 1.48. The PBI values for BBL and DS were estimated to be < 0.21 according to the linear correlation between PBI and SAC_{340} from a previous study.[46]

The highest CRS was 84.25 nmol mg-DOC^{-1} in DC, whereas the CRS levels in other samples were < 8 nmol mg-DOC^{-1}. The exceptionally high CRS in DC was possibly due to the presence of a waste treatment plant nearby. The CRS level in sewage effluent-impact waters (16-22 mg-DOC^{-1})[70] was relatively higher than that in unpolluted freshwaters (*i.e.* 4-8 nmol mg-total carbon^{-1}).[71]

Based on the property parameters in Table S1 (*i.e.* except the PBI values due to the missing data for BBL and DC), the DOM samples were statistically classified into three groups (*i.e.* cophenetic correlation coefficient ≥ 0.99) (Figure1). The first group included SRHA and LM (*i.e.* inconsistency coefficient = 0), which represents the allochthonous-dominant DOM based on the understanding of these sampling sites.[23,46] The second group included AMR, BL, and BBL. Within this group, the BL and BBL were most similar (*i.e.* inconsistency coefficient = 0), but distinct from AMR (*i.e.* inconsistency coefficient = 0.71). The second group represents the autochthonous-dominant DOM. The difference between AMR and the pair of BL and BBL can be explained by the relatively higher allochthonous signature in AMR. The autochthonous-dominant DOM was distinct from the allochthonous-dominant DOM (*i.e.* inconsistency coefficient = 1.03), which is due to their property contrasts. Briefly speaking, the autochthonous-dominant DOM is relatively more aliphatic, optically lighter, more proteinaceous and at lower molecular weight, whereas the allochthonous-dominant DOM is more aromatic, optically darker, more humic and at higher molecular weight, consistent with previous studies.[46,72] The third group only included the DC, which was remarkably different from any other DOM sample (*i.e.* inconsistency coefficient = 1.78), possibly because the DC is influenced by wastewater effluent.

It is noteworthy that the classification of DOM samples in this study is operational in a relative sense (*i.e.* autochthonous- vs. allochthonous-dominant) and mainly based on optical spectroscopic properties. The classification only served to better interpret the DOM variations. Nonetheless, the

optical spectroscopic properties between these three operationally-classified groups are distinct to express potential effects on metal binding.

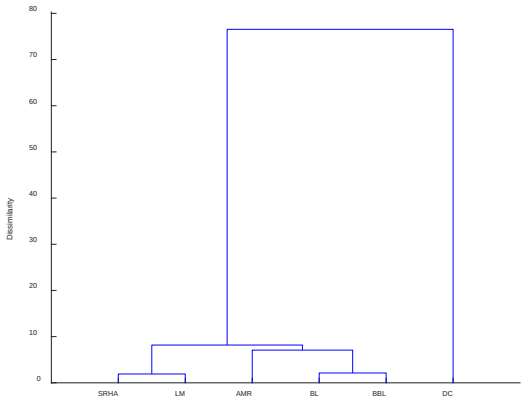

Figure 1 Dendrogram generated by hierarchical clustering analysis based on DOM properties in Table S1; Note: the PBI values were not included for making the dendrogram because of the missing data for BBL and DC

Dependence of metal binding on DOM sources

The metal binding curves (*i.e.* $C_{M,T}$ vs. C_M^{2+}) were compared between DOM samples (Figure 2). The Pb and Zn binding curves visually varied between DOM samples, but the variation was more substantial for Pb (Figure 2; left plot) than for Zn (Figure 2; middle plot). On the contrary, the Cd binding curves were relatively comparable across all DOM samples (Figure 2; right plot). Depending on the specific $C_{M,T}$, the variability in C_{Pb}^{2+}, C_{Zn}^{2+}, and C_{Cd}^{2+} ranged from 84- to 504-fold, 12- to 74-fold, and 2- to 14-fold, respectively between DOM samples (*i.e.* at similar $C_{M,T}$ the variability in C_M^{2+} = the highest C_M^{2+}/ the lowest C_M^{2+}; Table S2-S4). Triplicate binding experiments were only performed for Pb binding to SRHA, and the experimental uncertainty of C_{Pb}^{2+} was 1- to 3-time (*i.e.* at specific $C_{M,T}$ between triplicate experiments, the uncertainty of C_{Pb}^{2+} = the highest C_{Pb}^{2+} / the lowest C_{Pb}^{2+}). Assuming similar uncertainty level for Zn and Cd, the

variability in $C_M^{2+}$was generally larger than the experimental uncertainty, confirming that the observed difference in C_M^{2+} is attributed to variation of DOM sources (*i.e.* at fixed C_{DOC}, pH and ionic strength).

The dependency of metal binding on DOM source is metal-specific. The dependency is most substantial for Pb, relatively lower for Zn, and the smallest for Cd, indicating these three metals behave differently in response to DOM source variation, possibly due to different nature of metals for complexation. It is known that Pb principally chelates with organic ligands with salicylic- and/or catechol-type structures.[73,74] Therefore, the contrast of aromaticity, indicated by the $SUVA_{254}$ and SAC_{340} value, between our DOM samples results in distinct discrimination of Pb-binding. Zn and Cd show different preferences of functional groups from Pb for complexation. Zn mainly coordinates to a mixture of sulfur-, oxygen-/nitrogen- and oxygen-containing ligands in soil organic matter,[75,76] and Cd selectively coordinates to reduced sulfur group. These metal-specific preferences of organic ligands may explain the different levels of DOM effects between Pb, Zn, and Cd.

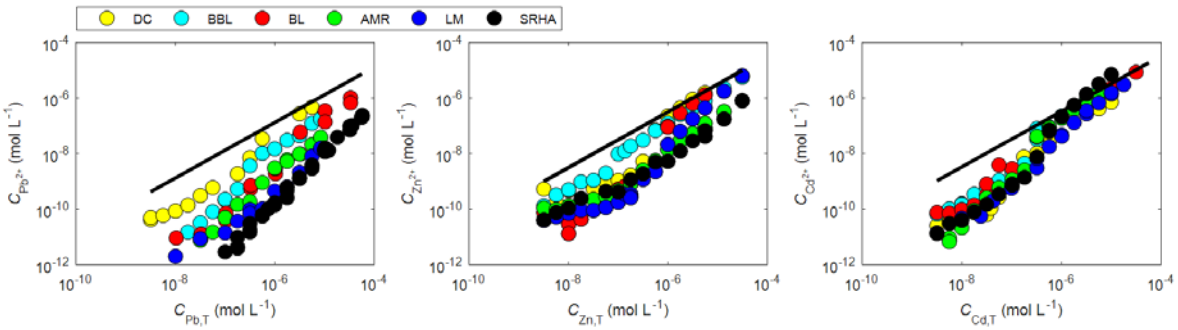

Figure 2 Influence of DOM on Pb, Zn and Cd binding at C_{DOC} = 10 mg L^{-1}, pH = 8.0 ± 0.1, and 0.1 mol L^{-1} KNO_3 electrolyte. The solid line corresponds to the blank in the absence of DOM. Circles in different colors indicates experimental data points. Triplicate experiments were only performed for SRHA.

The effects of DOM properties on F and WHAM performance

The effects of the F value on predicting C_{Pb}^{2+} by WHAM were evaluated. At F_{def} = 1.3, the agreements between the predicted and measured C_{Pb}^{2+} were generally better for SRHA, LM, and AMR ($RMSE_{def}$ = 0.79–0.97) than for other samples (Figure 3 and Table S5). The results indicated that F_{def} = 1.3 was more suitable to represent the active Pb-binding fraction in allochthonous DOM with high aromaticity ($SUVA_{254} \geq 14$, $SAC_{340} \geq 2.8$ and $SCOA_{436} \geq 1.45$ m^{-1} mg-C^{-1}). The F_{def} = 1.3, however, substantially overestimated the Pb binding to BBL and DC ($RMSE_{def}$ = 1.11–2.52) (Figure 3), which were relatively more autochthonous and less aromatic ($SUVA_{254} \leq 4.04$, $SAC_{340} \leq 0.86$, and $SCOA_{436} \leq 0.17$ L m^{-1} mg-C^{-1}). This contrast is reasonable given that much of the WHAM calibration data is based on isolated humic and fulvic acid.[16] The isolated compounds, however, only represent DOM with high allochthonous features, such as SRHA and LM. Optimizing F greatly improved in the case of autochthonous-dominant DOM (BL and BBL) and DC ($RMSE_{opt} \leq 0.58$), but only slightly improved for the allochthonous-dominant DOM (SRHA and LM) and AMR ($RMSE_{opt}$ = 0.57–0.82) (Table S5). The major source of $RMSE_{opt}$ was at $C_{Pb}^{2+} <$ 10^{-7} mol L^{-1}, where the measured C_{Pb}^{2+} was consistently higher than predicted C_{Pb}^{2+}, possibly because the measured C_{Pb}^{2+} was very close to the analytical detection limit ($10^{-11.6}$ mol L^{-1}) at low Pb:DOM ratio. The F_{opt} value increased from 0.03 to 1.9 in the following order: DC < BBL < BL < AMR < LM < SRHA (Table S5), indicating the active Pb-binding fraction in DOM increased as the DOM became increasingly allochthonous. Except the highest F_{opt} = 1.9 for SRHA, other F_{opt} values were smaller than F_{def} by 1.6–43 times (Table S5). Therefore, to achieve a reliable prediction of C_{Pb}^{2+} it was necessary to adjust the F value for site-specific DOM, particularly for the autochthonous DOMs with low aromaticity.

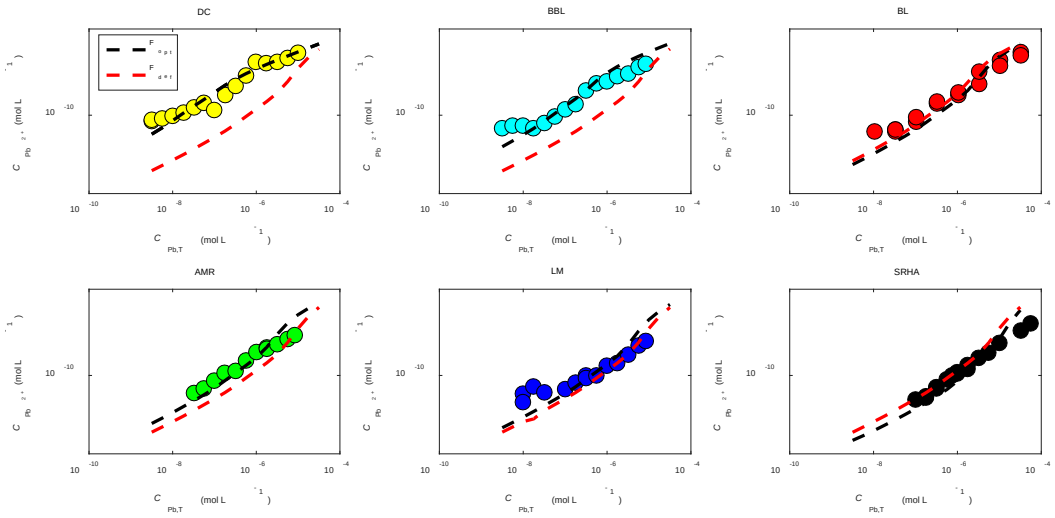

Figure 3 The influence of F_{opt} and F_{def} on predicting C_{Pb}^{2+}; Circles in different colors represent measured C_{Pb}^{2+} by AGNES for different samples.

The WHAM performance on predicting C_{Zn}^{2+} depended on the F value and DOM properties (Figure S7), but at a lesser extent compared to Pb. In most cases, better agreements were found between predicted and measured C_{Zn}^{2+} for the relatively more allochthonous DOM (*i.e.* LM and AMR; $RMSE_{def} \leq 0.80$) than for the autochthonous DOM (BBL and BL) and DC (*i.e.* $RMSE_{def} \geq 1.21$). The F_{opt} values substantially improved the prediction of C_{Zn}^{2+} for the autochthonous DOM (BL and BBL) and DC (*i.e.*,$RMSE_{opt} \leq 0.57$), but slightly improved for the allochthonous DOM (*i.e.* LM and AMR; $RMSE_{opt} \leq 0.78$). At $C_{Zn,T} \leq 10^{-8}$ mol L-1, the measured C_{Zn}^{2+} was consistently higher than the predicted C_{Zn}^{2+} for all samples, likely due the measured C_{Zn}^{2+} approaching to the detection limit. The F_{opt} values ranged from 0.10 to 1.00 (Table S5), congruent with previous studies (0.13–1.02).[26,36] The F_{opt} values were significantly smaller than F_{def} by a factor of 1.2–10.8, suggesting the adjustment of F for a better C_{Zn}^{2+} estimation.

The WHAM performance on predicting C_{Cd}^{2+} data were less sensitive to the F value and DOM variations than for Pb and Zn (Figure S8). The agreements between predicted and measured C_{Cd}^{2+}

were better at F_{def} = 1.3 than for Pb (Table S5; $RMSE_{def} \leq 0.83$). The prediction of C_{Cd}^{2+} at F_{def} was already acceptable for LM and DC ($RMSE_{def}$ = 0.23 and 0.38, respectively), and barely improved at F_{opt} ($RMSE_{opt}$ = 0.22 and 0.35, respectively). However, the improvements were more remarkable for SRHA, AMR, BL, and BBL ($RMSE_{opt} \leq 0.4$). The major source of RMSE mainly derived from the disagreements at $C_{Cd,T} \leq 10^{-8}$ mol L^{-1}, possibly due to C_{Cd}^{2+} measurements closed to detection limit. The F_{opt} values ranged from 0.30 to 1.10 (Table S5), wider than the F_{opt} range (*i.e.* 0.12–0.50) reported by Mueller *et al.*,[26] possibly because greater DOM variations in this study. All the F_{opt} values for Cd were smaller than the F_{def} by a factor of 1.2–4.3. This deviation from F_{def} was smaller than that for Pb (*i.e.* a factor of 1.6–43), indicating the F_{opt} for Cd was less dependent on DOM sources. Using the F_{def} = 1.3 for predicting $C_{Cd}^{2+}$was found to be acceptable.

Our results showed the F_{opt} value is DOM site-specific, as well as metal-specific. The F_{def} = 1.3 overpredicted the Pb and Zn binding to autochthonous DOM, which potentially caused the BLM to underestimate the Pb and Zn toxicity in the autochthonous waters. Therefore, adjusting F for the consideration of DOM variation is necessary.

Relate DOM properties to F_{opt}

Only a few studies[12,14,25,26] have explored the correlations between the F_{opt} values and the DOM optical properties (i.e. fluorescent components[14,2614,26] or $SUVA_{254}$ and SAC_{340}[12,25]). Most of these studies were limited to Cu,[12,14,25,26] and only one study was available for Zn and Cd[26] and none were found for Pb. More importantly, the derivation of F_{opt} values required the determination of C_M^{2+}. Because AGNES exclusively determines C_{Pb}^{2+},[33,35] C_{Zn}^{2+},[52] and C_{Cd}^{2+},[52] the determination of reliable F_{opt} can be achieved. Significant linear correlations were found between DOM properties (except PBI) and F_{opt} (Table S6).

For Pb, except Abs_{254}/Abs_{365}, S_R, C2, C3, and CRS ($p > 0.05$), the optical proxies showed significant linear correlations with F_{opt} (p = 0.003–0.042). The Hum/Pro and $SCOA_{436}$ showed relatively stronger linear correlations with F_{opt} (R^2 = 0.92 and 0.82) (Figure 4) than did other optical measures ($SUVA_{254}$, $SUVA_{340}$, FI, BIX and C1) (R^2 = 0.69–0.82). These combined results indicate that as the DOMs become more allochthonous, more humic-like, more aromatic, and optically darker, the active Pb-binding fraction increases. A similar trend has been observed for Cu in previous studies,[12,14,25,26] indicating Pb may compete with Cu for similar functional groups on aromatic structures. Coordination chemistry has shown Pb predominantly binds to the phenolic and carboxylic group on a salicylic-type structure or two adjacent carboxylic groups on catechol-type structure,[73,74] which explains the increasing F_{opt} with increasing aromaticity. The high PBI values in allochthonous DOM samples (PBI $\geq$ 0.72 for SRHA and LM; Table S1) also support this conclusion (*i.e.* the higher PBI, the stronger the expected metal binding). The insignificant correlations with Abs_{254}/Abs_{365} and S_R demonstrated that Pb binding was not affected by DOM molecular weight, contradictory to the marine DOM study[77] that observed different size-distributions of different Pb binding sites. Town *et al.*[16] also suggested the dependency of Pb concentration on freshwater size-fractionated DOM. These disagreements may be attributed to the sensitivity of Abs_{254}/Abs_{365} and S_R in response to molecular weight.

For Zn, no significant correlation between F_{opt} and DOM properties was found. When SRHA was not considered, the F_{opt} showed significant correlation with Abs_{254}/Abs_{365} and FI ($R^2 \geq 0.81$; $p \leq 0.03$) (Figure 4). The F_{opt} decreased with increasing Abs_{254}/Abs_{365} and FI, indicating the active Zn-binding fraction decreased as the DOM molecular weight decreased, and as the DOM source became less allochthonous. Contrarily, Muller *et al.*[26] reported the F_{opt} for Zn binding decreases with increasing allochthonous DOM feature (*i.e.* the humic-like component). Without explicit

knowledge of Zn binding sites (*e.g.* structures and compositions), it is impossible to assign F_{opt} to specific DOM properties. Coordination chemistry has shown that Zn binding to soil organic matter was through coordination with mixtures of sulfur (4–fold) and oxygen/nitrogen (6–fold) ligands in the first coordination shell.[75] The molecular structures of these ligands are possibly not aromatic, which explains the absence of correlations between F_{opt} and aromaticity (e.g. $SUVA_{254}$ and $SUVA_{340}$).

For Cd, when the full data set is considered, no significant linear correlation was found between DOM properties and F_{opt} ($p > 0.5$). When SRHA and DC are excluded as outliers, the F_{opt} value linearly increased with increasing $SUVA_{340}$ and $SCOA_{436}$ ($R^2 \geq 0.93$; $p \leq 0.04$) (Figure 4), indicating the active Cd-binding sites in these samples may reside on aromatic structures. The structures of Cd-binding sites in SRHA and DC, however, may be essentially different from aromatic features. The SRHA did not have the highest F_{opt}, although showing the highest $SUVA_{340}$ and $SCOA_{436}$. Contrarily, DC had the lowest $SUVA_{340}$ and $SCOA_{436}$, but having the second highest F_{opt}. Karlsson *et al.*[78] have found the Cd-binding sites in Suwannee River organic matter were mainly mixtures of oxygen/nitrogen and reduced sulfur ligands, and concluded the importance of reduced sulfur for coordination with Cd. The ligands in SRHA and DC, therefore, are possibly related to reduced sulfur with non-aromatic structures, which may explain why the highest aromaticity in SHRA did not correspond to the highest F_{opt}, and low aromaticity in DC corresponded to high F_{opt}. An alternative explanation of high F_{opt} in DC is the strong Cd binding to inorganic sulfide (*i.e.* CRS). Although WHAM did not include the thermodynamic stability constant for Cd binding to CRS, the amount of Cd-CRS can be still equivalently modeled by increasing the amount of bidentate and tridentate binding sites through the increase of F. Therefore, to account for the high CRS in DC (84.25 nmol mg-DOC^{-1}), high F_{opt} is required.

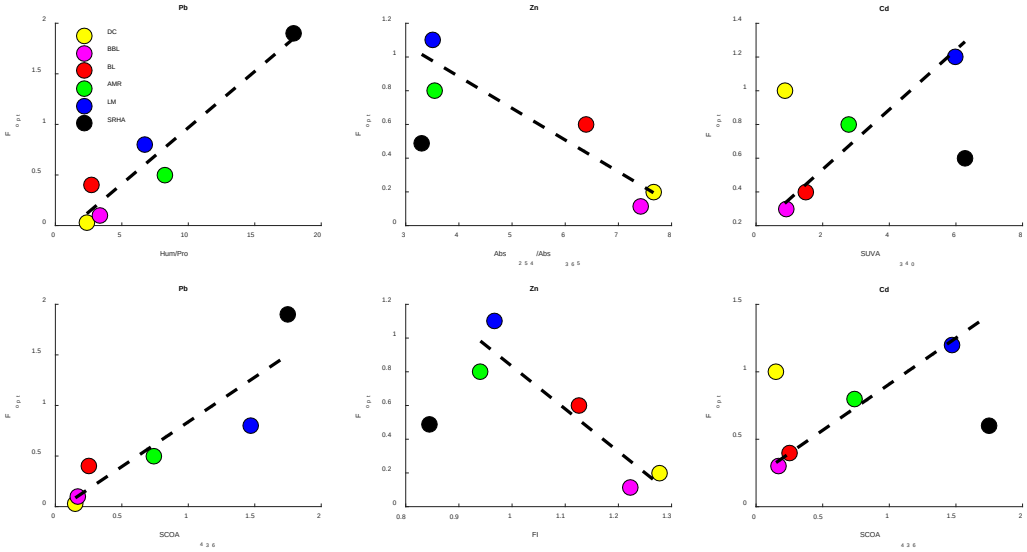

Figure 4 Linear correlations between different optical properties and F_{opt} for Pb, Cd, and Zn; Note: SRHA for Zn, and SRHA and DC for Cd, were not included in the linear regression analysis.

Potential to estimate F_{opt} for site-specific DOM using optical properties

Although the compositional and structural knowledge of organic ligands involved in metal binding is unknown, F_{opt} correlated with different property-indicators and the correlations were metal-specific. The correlations provide a potential to estimate F_{opt} for site-specific DOM based on simple measurement of optical properties.

For Pb, the aromaticity (Hum/Pro and $SCOA_{436}$) explained the variability of Pb-binding between different DOM samples.

For Zn, the F_{opt} values were influenced by the molecular weight, although the optical measurement may be not sensitive enough to differentiate molecular weights.

For Cd, the aromaticity may only partially account for Cd-binding variability. Reduced sulfur, including CRS and thiol, needs be considered because of their strong affinity to Cd. If the reduced sulfur groups are not associated with aromatic structure, it is not appropriate to use optical properties to estimate F_{opt}. The primary production by phytoplankton and macrophyte is the major

contributor of thiol in the autochthonous DOM pool.[72] Measuring the CRS and/thiol concentration in the autochthonous DOM, therefore, is important for predicting Cd speciation. However, for the highly allochthonous DOM, it is feasible to use optical properties to estimate F_{opt}.

Overall, F_{opt} quantitatively controls the metal binding site capacity, while the binding constant qualitatively regulates binding affinity (logK). The level of metal binding depends on ligand capacity and affinity. If only adjusting binding site capacity cannot fully explain metal binding variability induced by DOM source heterogeneity, adjusting the logK may be necessary. Future studies are required to evaluate how metal binding affinity varies between DOM samples.

ASSOCIATED CONTENT

Supporting Information

Descriptions of experimental procedures for FEEM, absorbance, potentiometric titration, and AGNES; method description for hierarchical analysis; model testing of the SO_4^{2-} effects on metal binding; table of $C_{M,T}$ vs. C_M^{2+} data; table of statistics of correlation between F_{opt} and DOM properties; figures of AGNES validation, FEEM, and proton binding affinity spectrum; This material as a PDF file is available free of charge via the Internet at http://pubs.acs.org.

Author information

Corresponding author

*Phone: +17057451011 ext 7859; Fax: +17057481625. E-mail: celinegueguen@trentu.ca.

Notes: The authors declare no competing financial interest.

Acknowledgement

This work was financially supported by the Canada Research Chairs program (for Celine Guéguen), and the Natural Sciences and Engineering Research Council of Canada (for Celine

Guéguen and D. Scott Smith). The authors also thank Dr. Chad Cuss for the help on data analysis. Three anonymous reviewers are also acknowledged for their constructive comments that help improve the manuscript.

REFERENCES

(1) Tait, T. N.; Cooper, C. A.; McGeer, J. C.; Wood, C. M.; Smith, D. S. Influence of dissolved organic matter (DOM) source on copper speciation and toxicity to Brachionus plicatilis. *Environ. Chem.* **2016**, *13* (3), 496–506.

(2) Allen, H. E.; Hall, R. H.; Brisbin, T. D. Metal speciation. Effects on aquatic toxicity. *Environ. Sci. Technol.* **1980**, *14* (4), 441–443.

(3) Sunda, W. G.; Engel, D. W.; Thuotte, R. M. Effect of chemical speciation on toxicity of cadmium to grass shrimp, Palaemonetes pugio: importance of free cadmium ion. *Environ. Sci. Technol.* **1978**, *12* (4), 409–413.

(4) Sánchez-Marín, P.; Santos-Echeandía, J.; Nieto-Cid, M.; Álvarez-Salgado, X. A.; Beiras, R. Effect of dissolved organic matter (DOM) of contrasting origins on Cu and Pb speciation and toxicity to Paracentrotus lividus larvae. *Aquat. Toxicol.* **2010**, *96* (2), 90–102.

(5) Tipping, E. Cation Binding by Humic Substances. *Cambridge Environmental Chemistry Series*. 2004, p 448.

(6) Leenheer, J. .; Croué, J. J.-P. Peer reviewed: characterizing aquatic dissolved organic matter. *Environ. Sci. Technol.* **2003**, *37* (1), 18A–26A.

(7) Minor, E. C.; Swenson, M. M.; Mattson, B. M.; Oyler, A. R. Structural characterization of dissolved organic matter: a review of current techniques for isolation and analysis. *Environ.*

Sci. Process. Impacts **2014**, *16* (9), 2064–2079.

(8) Karlsson, T.; Persson, P.; Skyllberg, U. Extended X-ray absorption fine structure spectroscopy evidence for the complexation of cadmium by reduced sulfur groups in natural organic matter. *Environ. Sci. Technol.* **2005**, *39* (9), 3048–3055.

(9) Karlsson, T.; Elgh-Dalgren, K.; Björn, E.; Skyllberg, U. Complexation of cadmium to sulfur and oxygen functional groups in an organic soil. *Geochim. Cosmochim. Acta* **2007**, *71* (3), 604–614.

(10) Smith, S.; Bell, R. A.; Kramer, J. R. Metal speciation in natural waters with emphasis on reduced sulfur groups as strong metal binding sites. *Comp. Biochem. Physiol. Part C Toxicol. Pharmacol.* **2002**, *133* (1–2), 65–74.

(11) Chen, W. B.; Smith, D. S.; Guéguen, C. Influence of water chemistry and dissolved organic matter (DOM) molecular size on copper and mercury binding determined by multiresponse fluorescence quenching. *Chemosphere* **2013**, *92* (4), 351–359.

(12) Chappaz, A.; Curtis, P. J. Integrating empirically dissolved organic matter quality for WHAM VI using the DOM optical properties: a case study of Cu-Al-DOM interactions. *Environ. Sci. Technol.* **2013**, *47* (4), 2001–2007.

(13) Stockdale, A.; Tipping, E.; Lofts, S. Dissolved trace metal speciation in estuarine and coastal waters: comparison of WHAM/Model VII predictions with analytical results. *Environ. Toxicol. Chem.* **2015**, *34* (1), 53–63.

(14) Ahmed, I. a M.; Hamilton-Taylor, J.; Bieroza, M.; Zhang, H.; Davison, W. Improving and testing geochemical speciation predictions of metal ions in natural waters. *Water Res.* **2014**,

493 *67C*, 276–291.

494 (15) Cheng, T.; Allen, H. E. Comparison of zinc complexation properties of dissolved natural
495 organic matter from different surface waters. *J. Environ. Manage.* **2006**, *80* (3), 222–229.

496 (16) Town, R. M.; Filella, M. Implications of natural organic matter binding heterogeneity on
497 understanding lead(II) complexation in aquatic systems. *Sci. Total Environ.* **2002**, *300* (1–
498 3), 143–154.

499 (17) Lofts, S.; Tipping, E. Assessing WHAM/Model VII against field measurements of free
500 metal ion concentrations: Model performance and the role of uncertainty in parameters and
501 inputs. *Environ. Chem.* **2011**, *8* (5), 501–516.

502 (18) Bryan, S. E.; Tipping, E.; Hamilton-Taylor, J. Comparison of measured and modelled
503 copper binding by natural organic matter in freshwaters. *Comp. Biochem. Physiol. - C*
504 *Toxicol. Pharmacol.* **2002**, *133* (1–2), 37–49.

505 (19) Baken, S.; Degryse, F.; Verheyen, L.; Merckx, R.; Smolders, E. Metal complexation
506 properties of freshwater dissolved organic matter are explained by its aromaticity and by
507 anthropogenic ligands. *Environ. Sci. Technol.* **2011**, *45* (7), 2584–2590.

508 (20) Crémazy, A.; Leclair, @bullet S; Mueller, @bullet K K; Vigneault, @bullet B; Campbell,
509 @bullet P G C; Fortin, @bullet C; Leclair, Á. S.; Campbell, Á. P. G. C.; Fortin, Á. C.;
510 Mueller, K. K. Development of an In Situ Ion-Exchange Technique for the Determination
511 of Free Cd, Co, Ni, and Zn Concentrations in Freshwaters. *Aquat Geochem* **2015**, *21*, 259–
512 279.

513 (21) Mueller, K. K.; Fortin, C.; Campbell, P. G. C. Spatial Variation in the Optical Properties of

514 Dissolved Organic Matter (DOM) in Lakes on the Canadian Precambrian Shield and Links
515 to Watershed Characteristics. *Aquat. Geochemistry* **2012**, *18* (1), 21–44.

516 (22) Luider, C. D.; Crusius, J.; Playle, R. C.; Curtis, P. J. Influence of Natural Organic Matter
517 Source on Copper Speciation As Demonstrated by Cu Binding to Fish Gills, by Ion
518 Selective Electrode, and by DGT Gel Sampler. *Environ. Sci. Technol.* **2004**, *38* (10), 2865–
519 2872.

520 (23) Richards, J. G.; Curtis, P. J.; Burnison, B. K.; Playle, R. C. Effects of natural organic matter
521 source on reducing metal toxicity to rainbow trout (Oncorhynchus mykiss) and on metal
522 binding to their gills. *Environ. Toxicol. Chem.* **2001**, *20* (6), 1159–1166.

523 (24) Schwartz, M. L.; Curtis, P. J.; Playle, R. C. INFLUENCE OF NATURAL ORGANIC
524 MATTER SOURCE ON ACUTE COPPER, LEAD, AND CADMIUM TOXICITY TO
525 RAINBOW TROUT (ONCORHYNCHUS MYKISS). *Environ. Toxicol. Chem.* **2004**, *23*
526 (12), 2889.

527 (25) De Schamphelaere, K. A. C.; Vasconcelos, F. M.; Tack, F. M. G.; Allen, H. E.; Janssen, C.
528 R. Effect of dissolved organic matter source on acute copper toxicity to Daphnia magna.
529 *Environ. Toxicol. Chem.* **2004**, *23* (5), 1248–1255.

530 (26) Mueller, K. K.; Lofts, S.; Fortin, C.; Campbell, P. G. C. Trace metal speciation predictions
531 in natural aquatic systems: Incorporation of dissolved organic matter (DOM) spectroscopic
532 quality. *Environ. Chem.* **2012**, *9* (4), 356–368.

533 (27) Macdonald, A.; Silk, L.; Schwartz, M.; Playle, R. C. A lead-gill binding model to predict
534 acute lead toxicity to rainbow trout (Oncorhynchus mykiss). *Comp. Biochem. Physiol.* **2002**,

133 (1–2), 227–242.

(28) Brix, K. V.; Esbaugh, A. J.; Munley, K. M.; Grosell, M. Investigations into the mechanism of lead toxicity to the freshwater pulmonate snail, Lymnaea stagnalis. *Aquat. Toxicol.* **2012**, *106–107*, 147–156.

(29) Besser, J. M.; Brumbaugh, W. G.; Brunson, E. L.; Ingersoll, C. G. Acute and chronic toxicity of lead in water and diet to the amphipod Hyalella azteca. *Environ. Toxicol. Chem.* **2005**, *24* (7), 1807–1815.

(30) Offem, B. O.; Ayotunde, E. O. Toxicity of Lead to Freshwater Invertebrates (Water fleas; Daphnia magna and Cyclop sp) in Fish Ponds in a Tropical Floodplain. *Water. Air. Soil Pollut.* **2008**, *192* (1–4), 39–46.

(31) Bringolf, R. B.; Morris, B. A.; Boese, C. J.; Santore, R. C.; Allen, H. E.; Meyer, J. S. Influence of dissolved organic matter on acute toxicity of zinc to larval fathead minnows (Pimephales promelas). *Arch. Environ. Contam. Toxicol.* **2006**, *51* (3), 438–444.

(32) De Schamphelaere, K. a C.; Lofts, S.; Janssen, C. R. Bioavailability models for predicting acute and chronic toxicity of zinc to algae, daphnids, and fish in natural surface waters. *Environ. Toxicol. Chem.* **2005**, *24* (5), 1190–1197.

(33) Pernet-Coudrier, B.; Companys, E.; Galceran, J.; Morey, M.; Mouchel, J. M.; Puy, J.; Ruiz, N.; Varrault, G. Pb-binding to various dissolved organic matter in urban aquatic systems: Key role of the most hydrophilic fraction. *Geochim. Cosmochim. Acta* **2011**, *75* (14), 4005–4019.

(34) Wu, J.; Zhang, H.; He, P. J.; Shao, L. M. Insight into the heavy metal binding potential of

556 dissolved organic matter in MSW leachate using EEM quenching combined with
557 PARAFAC analysis. *Water Res.* **2011**, *45* (4), 1711–1719.

558 (35) Puy, J.; Galceran, J.; Huidobro, C.; Companys, E.; Samper, N.; Garcés, J. L.; Mas, F.
559 Conditional Affinity Spectra of Pb 2+ −Humic Acid Complexation from Data Obtained
560 with AGNES. *Environ. Sci. Technol.* **2008**, *42* (24), 9289–9295.

561 (36) Cheng, T.; Schamphelaere, K. De; Lofts, S.; Janssen, C.; Allen, H. E. Measurement and
562 computation of zinc binding to natural dissolved organic matter in European surface waters.
563 *Anal. Chim. Acta* **2005**, *542* (2), 230–239.

564 (37) Xue, H.; Sigg, L. Cadmium speciation and complexation by natural organic ligands in fresh
565 water. *Anal. Chim. Acta* **1998**, *363* (2–3), 249–259.

566 (38) Xue, H.; Sigg, L. Comparison of the complexation of Cu and Cd by humic or fulvic acids
567 and by ligands observed in lake waters. *Aquat. Geochemistry* **1999**, *5* (4), 313–335.

568 (39) Rey-Castro, C.; Mongin, S.; Huidobro, C.; David, C.; Salvador, J.; Garcés, J. L.; Galceran,
569 J.; Mas, F.; Puy, J. Effective affinity distribution for the binding of metal ions to a generic
570 fulvic acid in natural waters. *Environ. Sci. Technol.* **2009**, *43* (19), 7184–7191.

571 (40) Pesavento, M.; Alberti, G.; Biesuz, R. Analytical methods for determination of free metal
572 ion concentration, labile species fraction and metal complexation capacity of environmental
573 waters: A review. *Analytica Chimica Acta*. 2009, pp 129–141.

574 (41) Xue, H. B.; Jansen, S.; Prasch, A.; Sigg, L. Nickel speciation and complexation kinetics
575 freshwater by ligand exchange and DPCSV. *Environ. Sci. Technol.* **2001**, *35* (3), 539–546.

576 (42) Hudson, N.; Baker, A.; Reynolds, D. Fluorescence analysis of dissolved organic matter in

577 natural, waste and polluted waters - A review. *River Research and Applications*. 2007, pp
578 631–649.

579 (43) Weishaar, J. L.; Aiken, G. R.; Bergamaschi, B. a.; Fram, M. S.; Fujii, R.; Mopper, K.
580 Evaluation of specific ultraviolet absorbance as an indicator of the chemical composition
581 and reactivity of dissolved organic carbon. *Environ. Sci. Technol.* **2003**, *37* (20), 4702–
582 4708.

583 (44) Helms, J. R.; Stubbins, A.; Ritchie, J. D.; Minor, E. C.; Kieber, D. J.; Mopper, K. Absorption
584 spectral slopes and slope ratios as indicators of molecular weight, source, and
585 photobleaching of chromophoric dissolved organic matter. *Limonology Oceanogr.* **2008**, *53*
586 (3), 955–969.

587 (45) Smith, D. S.; Ferris, F. G. Proton binding by hydrous ferric oxide and aluminum oxide
588 surfaces interpreted using fully optimized continuous pka spectra. *Environ. Sci. Technol.*
589 **2001**, *35* (23), 4637–4642.

590 (46) Al-Reasi, H. A.; Wood, C. M.; Smith, D. S. Characterization of freshwater natural dissolved
591 organic matter (DOM): Mechanistic explanations for protective effects against metal
592 toxicity and direct effects on organisms. *Environ. Int.* **2013**, *59*, 201–207.

593 (47) Bowles, K. C.; Ernste, M. J.; Kramer, J. R. Trace Sulfide Determination in Oxic
594 Freshwaters. *Anal. Chim. Acta* **2003**, *477* (1), 113–124.

595 (48) Kramer, J. R.; Bell, R. A.; Smith, D. S. Determination of sulfide ligands and association
596 with natural organic matter. *Appl. Geochemistry* **2007**, *22* (8), 1606–1611.

597 (49) Smith, D. S.; Bell, R. a.; Kramer, J. R. Metal speciation in natural waters with emphasis on

598 reduced sulfur groups as strong metal binding sites. *Comp. Biochem. Physiol. - C Toxicol.*
599 *Pharmacol.* **2002**, *133* (1–2), 65–74.

600 (50) Town, R. M.; Filella, M. Dispelling the myths: Is the existence of L1 and L2 ligands
601 necessary to explain metal ion speciation in natural waters? *Limnology and Oceanography*.
602 2000, pp 1341–1357.

603 (51) Galceran, J.; Companys, E.; Puy, J.; Cecilia, J.; Garces, J. L. AGNES: A new
604 electroanalytical technique for measuring free metal ion concentration. *J. Electroanal.*
605 *Chem.* **2004**, *566* (1), 95–109.

606 (52) Companys, E.; Puy, J.; Galceran, J. Humic acid complexation to Zn and Cd determined with
607 the new electroanalytical technique AGNES. *Environ. Chem.* **2007**, *4* (5), 347–354.

608 (53) Sun, L.; Perdue, E. M.; McCarthy, J. F. Using reverse osmosis to obtain organic matter from
609 surface and ground waters. *Water Res.* **1995**, *29* (6), 1471–1477.

610 (54) Al-Reasi, H. A.; Wood, C. M.; Smith, D. S. Physicochemical and spectroscopic properties
611 of natural organic matter (NOM) from various sources and implications for ameliorative
612 effects on metal toxicity to aquatic biota. *Aquat. Toxicol.* **2011**, *103* (3–4), 179–190.

613 (55) Chen, W.; Westerhoff, P.; Leenheer, J. A.; Booksh, K. Fluorescence Excitation-Emission
614 Matrix Regional Integration to Quantify Spectra for Dissolved Organic Matter. *Environ.*
615 *Sci. Technol.* **2003**, *37* (24), 5701–5710.

616 (56) McKnight, D. M.; Boyer, E. W.; Westerhoff, P. K.; Doran, P. T.; Kulbe, T.; Andersen, D.
617 T. Spectrofluorometric characterization of dissolved organic matter for indication of
618 precursor organic material and aromaticity. *Limnol. Oceanogr.* **2001**, *46* (1), 38–48.

(57) Huguet, A.; Vacher, L.; Relexans, S.; Saubusse, S.; Froidefond, J. M.; Parlanti, E. Properties of fluorescent dissolved organic matter in the Gironde Estuary. *Org. Geochem.* **2009**, *40* (6), 706–719.

(58) Al-Reasi, H. a.; Wood, C. M.; Smith, D. S. Characterization of freshwater natural dissolved organic matter (DOM): Mechanistic explanations for protective effects against metal toxicity and direct effects on organisms. *Environ. Int.* **2013**, *59*, 201–207.

(59) Al-Reasi, H. A.; Smith, D. S.; Wood, C. M. Evaluating the ameliorative effect of natural dissolved organic matter (DOM) quality on copper toxicity to daphnia magna: Improving the BLM. *Ecotoxicology* **2012**, *21* (2), 524–537.

(60) Smith, D. S.; Kramer, J. R. Multi-site proton interactions with natural organic matter. *Environ. Int.* **1999**, *25* (2–3), 307–314.

(61) Craven, A. M.; Aiken, G. R.; Ryan, J. N. Copper(II) binding by dissolved organic matter: importance of the copper-to-dissolved organic matter ratio and implications for the biotic ligand model. *Environ. Sci. Technol.* **2012**, *46* (18), 9948–9955.

(62) Filella, M.; Town, R. M. A framework for interpretation and prediction of the effects of natural organic matter heterogeneity on trace metal speciation in aquatic systems. In *Environmental Chemistry: Green Chemistry and Pollutants in Ecosystems*; 2005; pp 121–132.

(63) Canadian Council of Ministers of the Enviroment. *Canadian Water Quality Guidelines for the Protection of Aquatic Life NITRATE ION*; 2012.

(64) Canada, H. *Guidelines for Canadian Drinking Water Quality: Guideline Technical*

Document – Sulphate; 1994.

(65) Buffle, J. Complexation Reactions in Aquatic Systems; Analytical Approach. In *Ellis Horwood Ltd*; WILEY –VCH Verlag GmbH, 1989; Vol. 17,

(66) Coble, P. G.; Lead, J.; Baker, A.; Reynolds, D.; Spencer, R. G. . *Aquatic Organic Matter Fluorescence*; Coble, P., Lead, J., Baker, A., Reynolds, D. M., Spencer, R. G. M., Eds.; Cambridge University Press: Cambridge, 2014.

(67) Abbt-Braun, G.; Frimmel, F. H. Basic characterization of Norwegian NOM samples - Similarities and differences. *Environ. Int.* **1999**, *25* (2–3), 161–180.

(68) Helms, J. R.; Stubbins, A.; Ritchie, J. D.; Minor, E. C.; Kieber, D. J.; Mopper, K. Absorption spectral slopes and slope ratios as indicators of molecular weight, source, and photobleaching of chromophoric dissolved organic matter. *Limnol. Oceanogr.* **2008**, *53* (3), 955–969.

(69) Inamdar, S.; Finger, N.; Singh, S.; Mitchell, M.; Levia, D.; Bais, H.; Scott, D.; McHale, P. Dissolved organic matter (DOM) concentration and quality in a forested mid-Atlantic watershed, USA. *Biogeochemistry* **2012**, *108* (1–3), 55–76.

(70) Smith, D. S.; Bell, R. A.; Valliant, J.; Kramer, J. R. Determination of Strong Ligand Sites in Sewage Effluent-Impacted Waters by Competitive Ligand Titration with Silver. *Environ. Sci. Technol.* **2004**, *38* (7), 2120–2125.

(71) Bowles, K. C.; Ernste, M. J.; Kramer, J. R. Trace sulfide determination in oxic freshwaters. *Anal. Chim. Acta* **2003**, *477* (1), 113–124.

(72) Toming, K.; Tuvikene, L.; Vilbaste, S.; Agasild, H. Contributions of autochthonous and

661 allochthonous sources to dissolved organic matter in a large, shallow, eutrophic lake with a
662 highly calcareous catchment. *Limnol. Ocean.* **2013**, *58* (4), 1259–1270.

663 (73) Xiong, J.; Koopal, L. K.; Tan, W.; Fang, L.; Wang, M.; Zhao, W.; Liu, F.; Zhang, J.; Weng,
664 L. Lead binding to soil fulvic and humic acids: NICA-donnan modeling and XAFS
665 spectroscopy. *Environ. Sci. Technol.* **2013**, *47* (20), 11634–11642.

666 (74) Manceau, A.; Boisset, M. C.; Sarret, G.; Hazemann, J. L.; Mench, M.; Cambier, P.; Prost,
667 R. Direct determination of lead speciation in contaminated soils by EXAFS spectroscopy.
668 *Environ. Sci. Technol.* **1996**, *30* (5), 1540–1552.

669 (75) Karlsson, T.; Skyllberg, U. Complexation of zinc in organic soils - EXAFS evidence for
670 sulfur associations. *Environ. Sci. Technol.* **2007**, *41* (1), 119–124.

671 (76) Xia, K.; Bleam, W.; Helmke, P. a. Studies of the nature of binding sites of first row transition
672 elements bound to aquatic and soil humic substances using X-ray absorption spectroscopy.
673 *Geochim. Cosmochim. Acta* **1997**, *61* (11), 2223–2235.

674 (77) Wells, M. L.; Kozelka, P. B.; Bruland, K. W. The complexation of `dissolved' Cu, Zn, Cd
675 and Pb by soluble and colloidal organic matter in Narragansett Bay, RI. *Mar. Chem.* **1998**,
676 *62* (3–4), 203–217.

677 (78) Karlsson, T.; Persson, P.; Skyllberg, U. Extended X-ray absorption fine structure
678 spectroscopy evidence for the complexation of cadmium by reduced sulfur groups in natural
679 organic matter. *Environ. Sci. Technol.* **2005**, *39* (9), 3048–3055.

680